SUPPLEMENTARY INFORMAION

SUPPLEMENTARY FIGURES AND LEGENDS

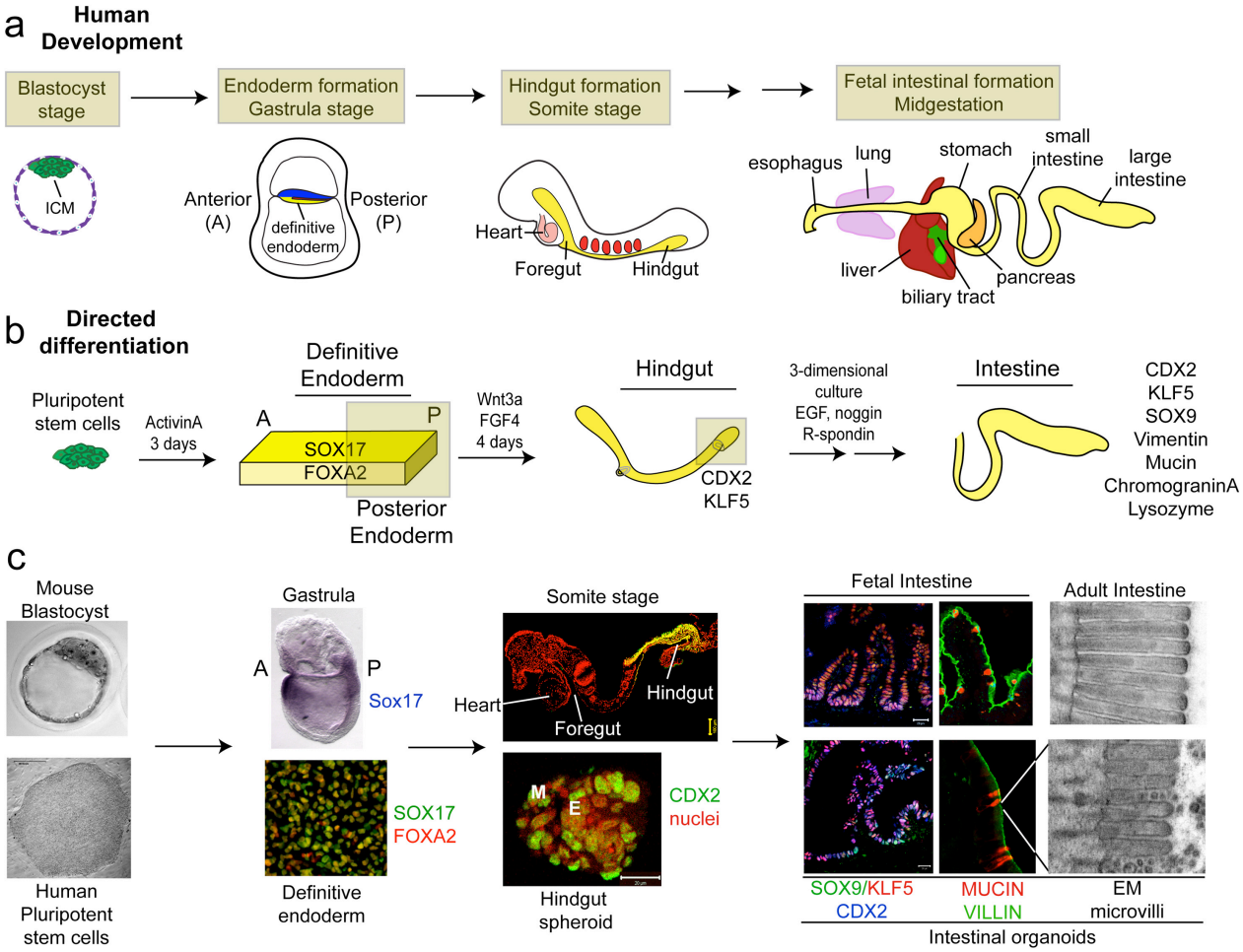

Supplementary Figure 1. Model comparing embryonic intestinal development versus directed differentiation of human PSCs into intestinal tissue *in vitro*.
a, Schematic of human intestinal development. At the blastocyst stage, the inner cell mass (ICM) gives rise to the entire embryo. The ICM is also the source of embryonic stem cells. At the gastrula stage, the embryo contains the three germ layers including the embryonic/definitive endoderm (yellow). The definitive endoderm forms a primitive gut tube, with the hindgut forming in the posterior region of the embryo. The hindgut undergoes intestinal morphogenesis forming the small and large intestines. **b,** Schematic of directed differentiation of PSCs into intestinal tissue. PSCs cultured for 3 days in ActivinA form definitive endoderm (DE) co-expressing SOX17 and FOXA2. DE cultured for 4 days in FGF4 and Wnt3a (500ng/ml each) form three-dimensional hindgut spheroids expressing the posterior marker CDX2. Spheroids formed intestinal organoids when grown in three dimensional conditions that favor expansion and differentiation of intestinal precursors (matrigel with 500ng/mL R-Spondin1, 100ng/mL Noggin and 50ng/mL EGF. **c,** Side-by-side comparison of embryonic intestinal development (top) and human intestinal organoid development (bottom). PSCs underwent staged differentiation in a manner that was highly reminiscent of embryonic intestinal development and formed intestinal tissue. Stages of development in **c** are meant to approximate the ones schematically shown in **a** and **b**. Mouse embryos were used for comparison because human embryonic images were not available.

Supplementary Figure 2. Efficiency of DE, hindgut, and intestinal differentiation.

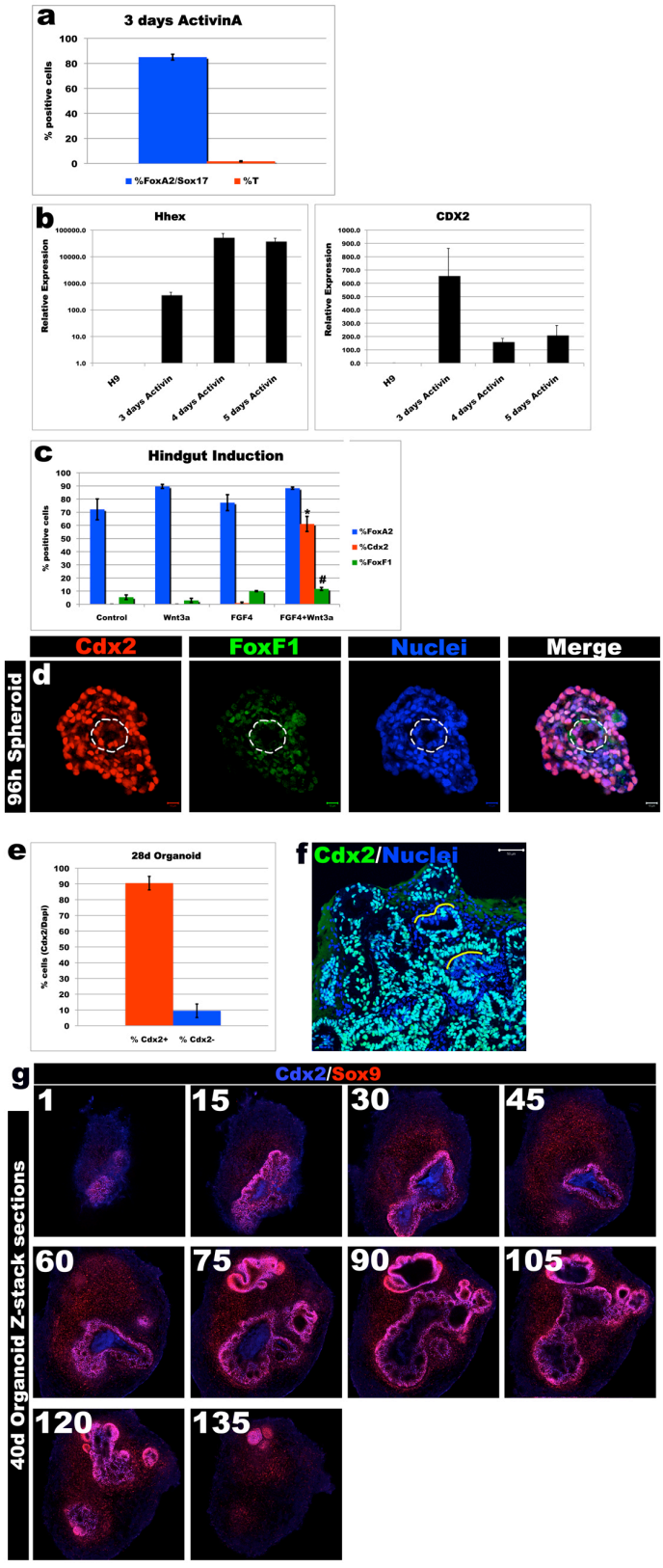

a, Efficiency of definitive endoderm (DE) (FOXA2/SOX17 double +) or mesoderm (T/Brachyury+) formation was assessed using immunohistochemistry. After 3 days, ActivinA treated cultures were 85% DE whereas 1.7% of cells were mesoderm. **b,** Activin treatment for 4-5 days results in DE that was anterior in character (HHEX+) and had reduced levels of CDX2 expression compared to 3 days of Activin treatment. **c,** Quantification of endoderm (FOXA2+), hindgut (intestine) (CDX2+) and mesoderm (FOXF1+) in monolayers following the hindgut induction protocol. There was an increase in mesoderm in all conditions compared to (a). In conditions where FGF4 was present, mesoderm expansion was enhanced (5.3% control vs. 10% FGF4 only, 11.7% FGF4+Wnt3a). CDX2 was significantly enhanced in FGF4+Wnt3a treated monolayers. **d,** Hindgut spheroids showed ubiquitous epithelial and mesenchymal expression of CDX2 (red). FOXF1 was weakly expressed in the mesenchyme and excluded from the epithelium (dashed line outlines endoderm). **e and f,** The efficiency for generating intestinal epithelia was quantified (n= 3 different organoids) by counting for CDX2+ and CDX2- nuclei. 90.5% of the epithelium was CDX2+ and 9.5% of the epithelium was CDX2- (e and f). Yellow lines in (f) highlight rare patches within the epithelium that are CDX2-. **g,** Whole mount immunohistochemistry for SOX9 and CDX2 on 28 and 40-day organoids (n = 5, representative organoid at 40 days shown). Images were captured through the entire organoid using confocal microscopy (z-series images captured every 2.5 microns). Representative sections through an entire organoid (every 15 slices shown, 37.5 microns between slices) demonstrates that the epithelium is almost entirely intestinal CDX2+) and SOX9 is restricted to the peripheral epithelium. All error bars are S.E.M.

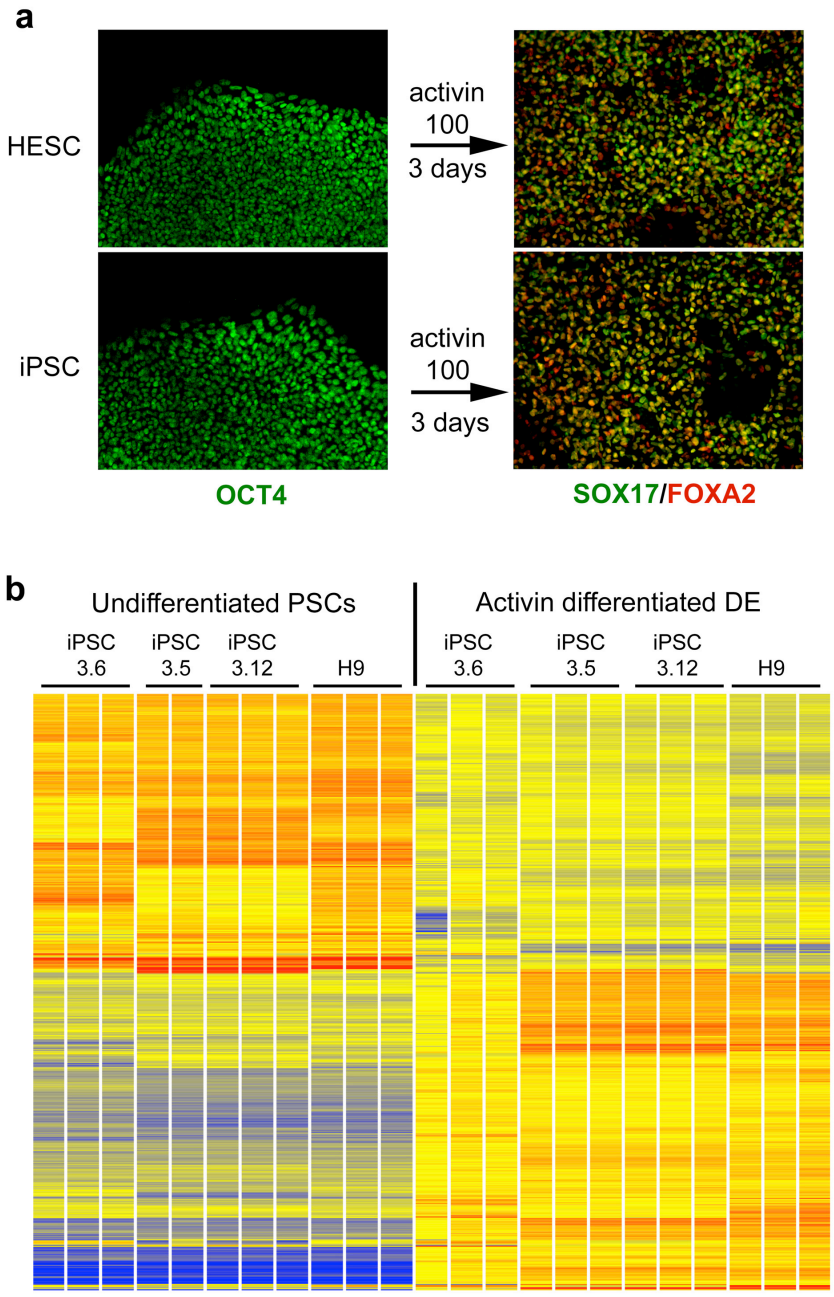

Supplementary Figure 3. Characterization of DE formation from HESC and iPSC lines by IF and Microarray analysis.

a, Undifferentiated HESCs stained with the pluripotency marker OCT4 (green) were treated for 3 days with ActivinA. This DE induction protocol routinely results in 80-90% SOX17 (green)/FOXA2 (red) double positive cells in both HESC and iPSC lines. **b,** Transcriptional profile of DE induction. HESC-H9 and iPSC lines 3.5, 3.6 and 3.12 were analyzed before and after DE formation (activin differentiation) by Affymetrix DNA microarray analysis. Clustering analysis of transcripts that were differentially regulated during DE formation indicated that iPSC lines 3.5 and 3.12 differentiate in a manner that is highly similar to HESC-H9 cells (see Supplementary table 1 for gene list and fold expression changes). iPSC line 3.6 had a more divergent transcriptional profile and was therefore not used for subsequent experiments.

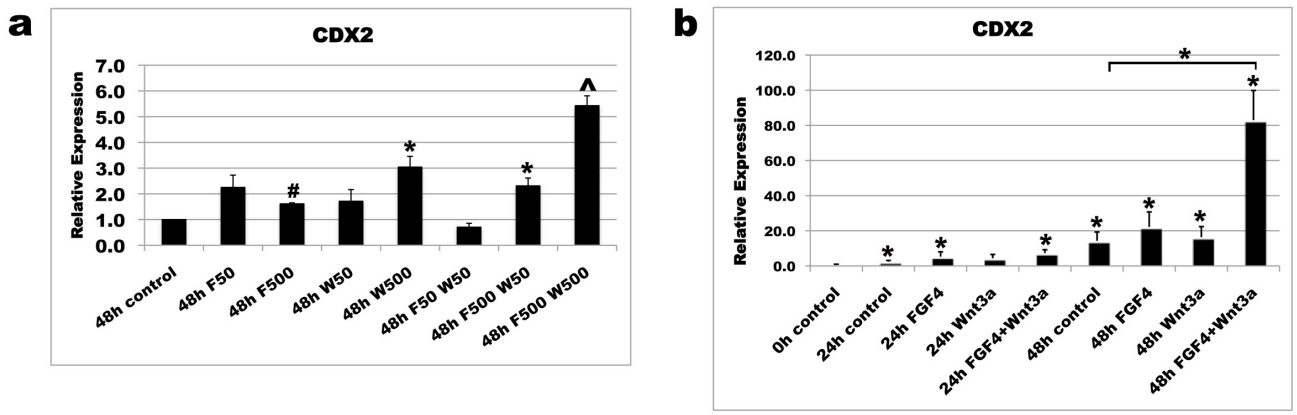

Supplementary Figure 4. Time and concentration dependent induction of CDX2 by FGF4 and Wnt3a. a, FGF4 and Wnt3a up-regulate CDX2 in a concentration dependant manner. 3-day ActivinA treated hESCs were treated for 48 hours with Wnt3a at 50ng/mL or 500ng/mL or FGF4 at 50ng/mL or 500ng/mL, or both FGF4+Wnt3a. Cells were analyzed after 48 hours of treatment. FGF4 or Wnt3a alone caused modest changes in CDX2 expression at different doses. FGF4+Wnt3a at the highest dose (500ng/mL each) induced robust CDX2 expression. CDX2 expression was normalized to the internal control beta-tubulin, and is shown relative to a 48 hour control cultured in the absence of growth factors. **b,** FGF4 and Wnt3a up-regulate CDX2 in a time dependant manner. 48 hours of exposure to FGF4+Wnt3a had the highest induction of CDX2. All time points shown are set relative to a 0 hour no growth factor control. 500ng/mL of FGF4, Wnt3a or FGF4+Wnt3a was used for all time points. Note that 24 hour and 48 controls, in the absence of growth factors, show a significant and spontaneous upregulation of CDX2. Error bars denote S.E.M (n=3). Significance is shown by; * ($p<0.05$)

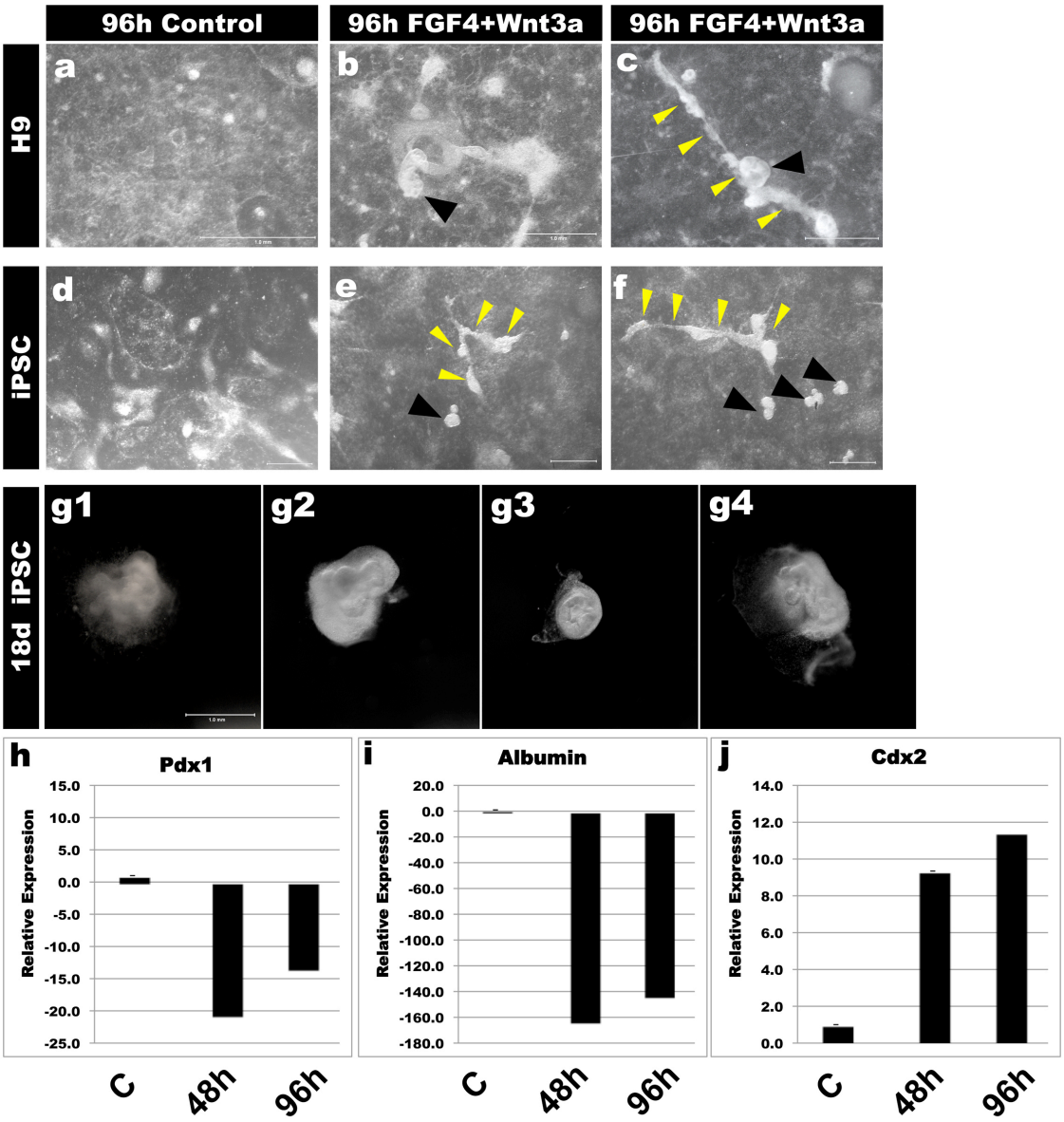

Supplementary Figure 5. Morphologic comparison of HESC and iPSC organoid formation and differentiation analysis of hindgut spheroids.

a-f, Hindgut spheroid formation from H9 human ESCs (a-c) or iPSCs (d-f) that were differentiated into endoderm and cultured without growth factors (a,d), or with 500ng/mL FGF4+Wnt3a (b,c,e,f) for 96 hours. Control cultures contained little evidence of three-dimensional structures (a,d) whereas FGF4+Wnt3a treated cultures contained tube-like structures (yellow arrowheads; c,e,f) and free floating spheroids (black arrowheads; b,c,e,f). **g,** Examples of four different iPSC spheroids that were expanded in matrigel for 18 days (g,1-4). As with HESC-derived organoids, iPSC organoids contain an internal epithelium surrounded by mesenchyme. **h-j,** RT-qPCR analysis of hindgut-like spheroids detected robust expression CDX2 but no expression of foregut markers (PDX1, Albumin). Expression levels shown in **h-j)** are relative to 3-day activin treated DE cultures that were grown for identical lengths of time in the absence of FGF4 or Wnt3a (C = control; 48h = spheroids generated after 48 hours; 96h = spheroids generated after 96 hours). Error bars denote S.E.M. n=3.

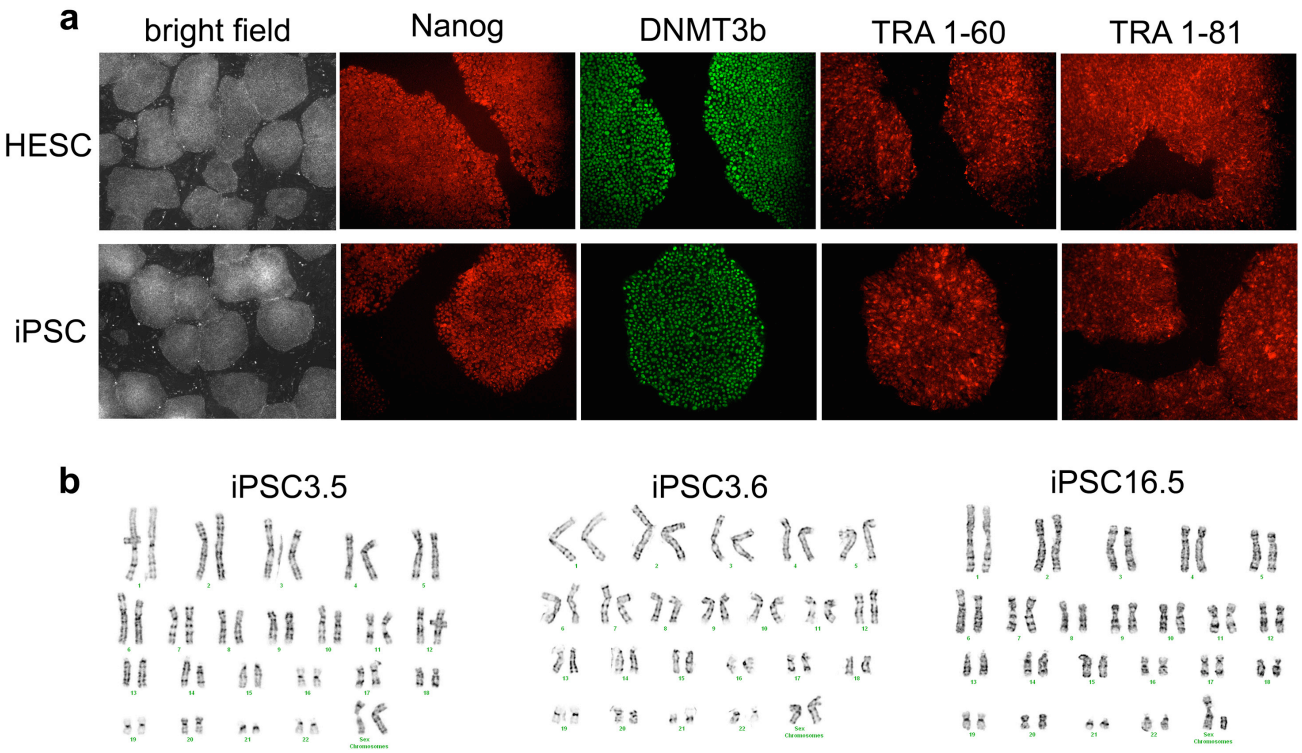

Supplementary Figure 6. Characterization of induced pluripotent stem cell lines.
All iPSC lines were compared to either HESC-H9 or HESC-H1 for morphology, pluripotency marker expression and karyotype. **a,** Example of HESC and iPSC morphology and expression of pluripotency markers NANOG, DNMT3b, TRA 1-60 and TRA 1-81. **b,** Examples of karyotypic analysis of iPSC lines 3.5, 3.6 and 16.5.

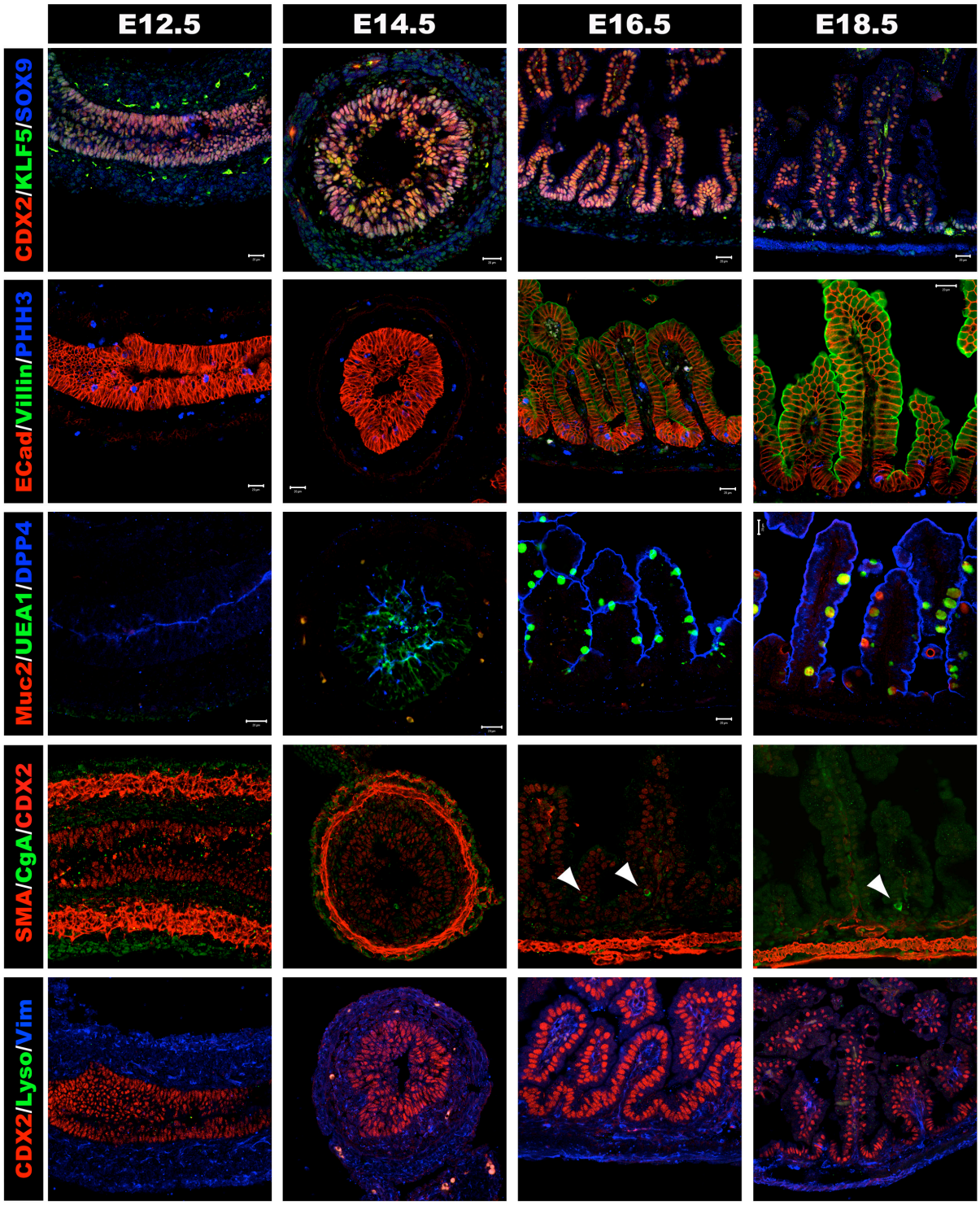

Supplementary Figure 7. Molecular marker expression during mouse intestinal development. Embryonic stages include e12.5, e14.5, e16.5 and e18.5. Transcription factors detected were CDX2, KLF5, and SOX9. Epithelial markers used were E-cadherin (Ecad), Villin and DPP4. Vimentin (Vim) and Smooth Muscle Actin (SMA) were used as a mesenchymal markers. Differentiation markers used were Lysozyme (Lyso) for paneth cells, Mucin (Muc2) and UEA-1 for goblet cells, Chromogranin A (CgA) for enteroendocrine cells. Phosphohistone H3 (PHH3) shows mitotic cells.

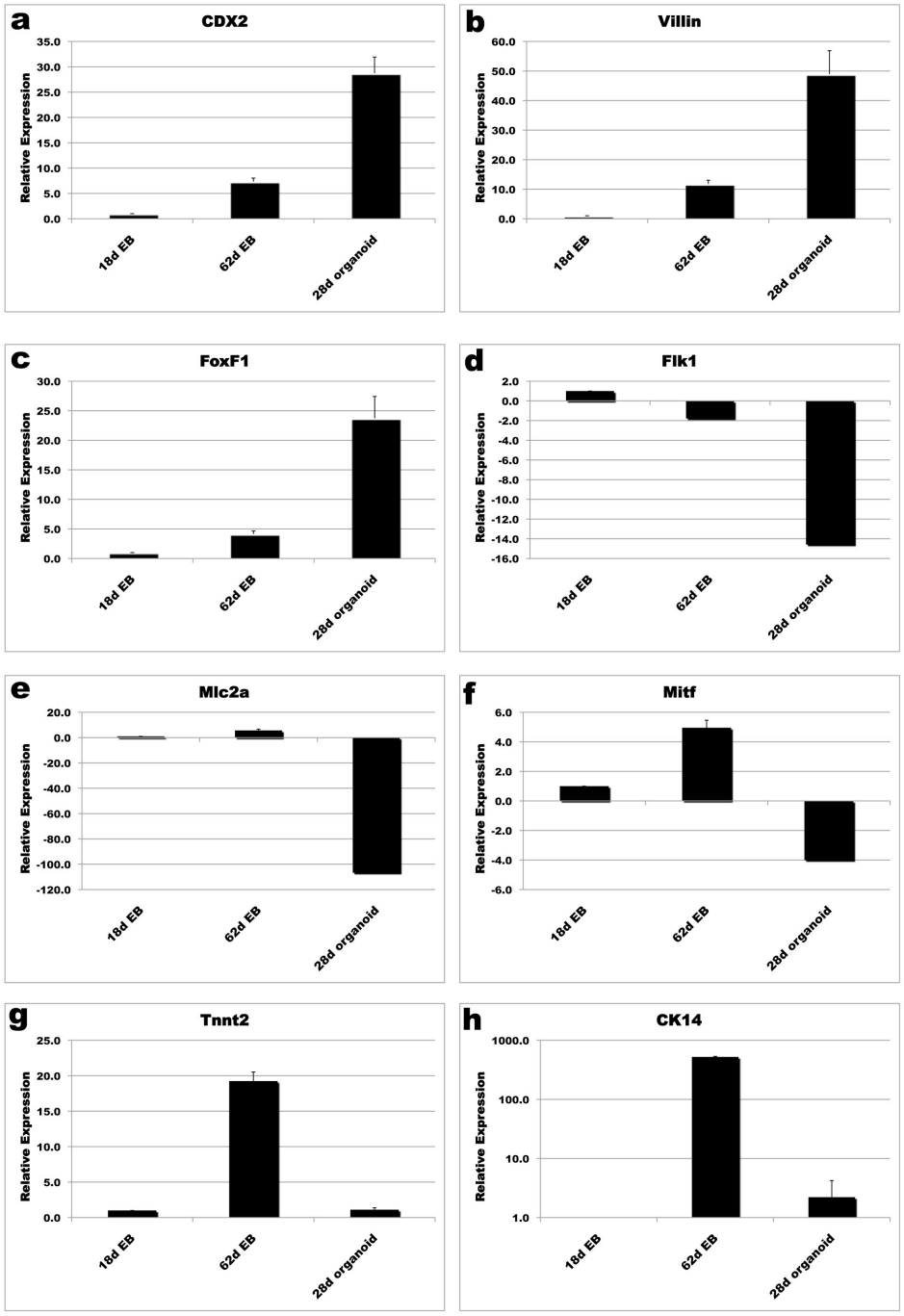

Supplementary Figure 8. qRT-PCR comparison between 28-day intestinal organoids and Embryoid Bodies (EBs).

a-h, EBs were generated and RNA was harvested after 18 days and 62 days and compared to RNA from 28-day intestinal organoids by qRT-PCR. All tissues were generated using H9 hESCs. Intestinal epithelial markers CDX2 and Villin (a and b) were 30-50 fold higher in Organoids compared to 18-day EBs and 5-fold higher than 62-day EBs. Similarly, the intestinal mesenchyme marker FoxF1 was dramatically increased in 28-day intestinal organoids (c). Intestinal organoids contained only intestinal tissue, whereas EBs contained a mix of tissues as was shown with the vascular marker Flk1 (d), the cardiac markers Mlc2a and Tnnt2 (e and g), the pigmented epithelium/melanocyte marker Mitf (f) and the keratinocyte marker CK14 (h). Error bars are S.E.M. n>=3 for each condition.

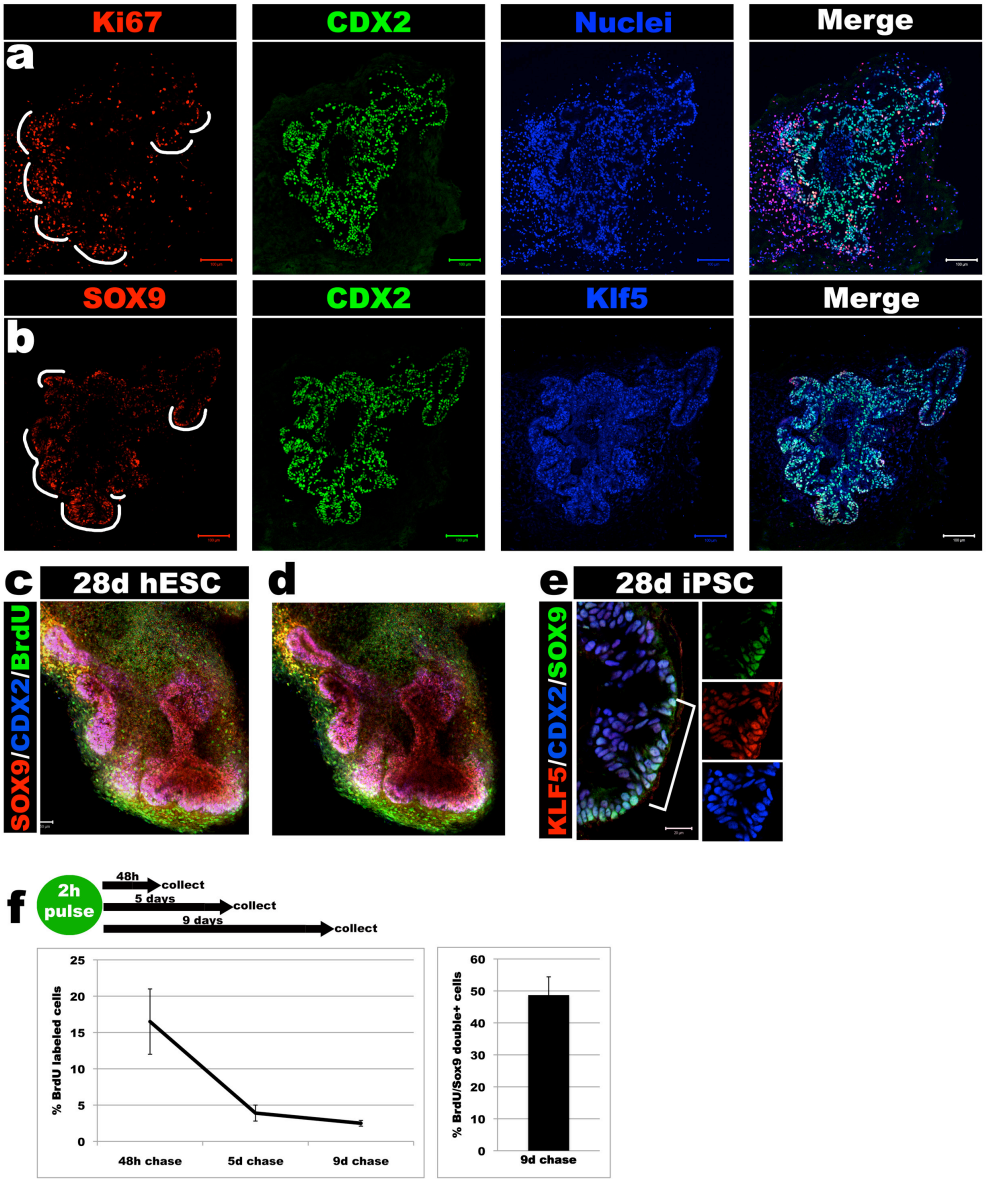

Supplementary Figure 9. Proliferation is restricted to discrete domains in intestinal organoids. **a and b,** Low magnification serial sections of a 28 day organoid (H9 hESC derived) demonstrating discrete domains of elevated proliferation **(a)** (Ki67, red, domains highlighted with white outline). Epithelial domains showing elevated levels of proliferation in (a) occur in SOX9 expression domains **(b)** (SOX9, red, domains highlighted with white outline). **c and d,** 2-dimensional rendering of a whole mount z-stack of a 28 day organoid co-stained with SOX9 (red), CDX2 (blue) and BrdU (green) showing epithelial proliferation in the SOX9 domain. **d,** shows a single slice through the center of the z-stack for increased cellular resolution. **e,** Human iPSCs derived from keratinocytes form intestinal organoids in an identical manner to HESCs as measured by KLF5, CDX2, and localized SOX9 expression. The insets to the right in e show separated color channels. **f,** A BrdU pulse-case experiment demonstrates rapid cellular expansion and turnover after 5 days (right). Organoids were labeled for two hours with BrdU and collected after 48 hours, 5 days and 9 days. The percent of BrdU+ intestinal epithelium was determined at each time point and steadily decreased. After 9 days 2.5% of the epithelium was BrdU+ and nearly half of these label-retaining cells resided in the SOX9 domain (right). Error bars denote S.E.M. n>=3 for each time point.

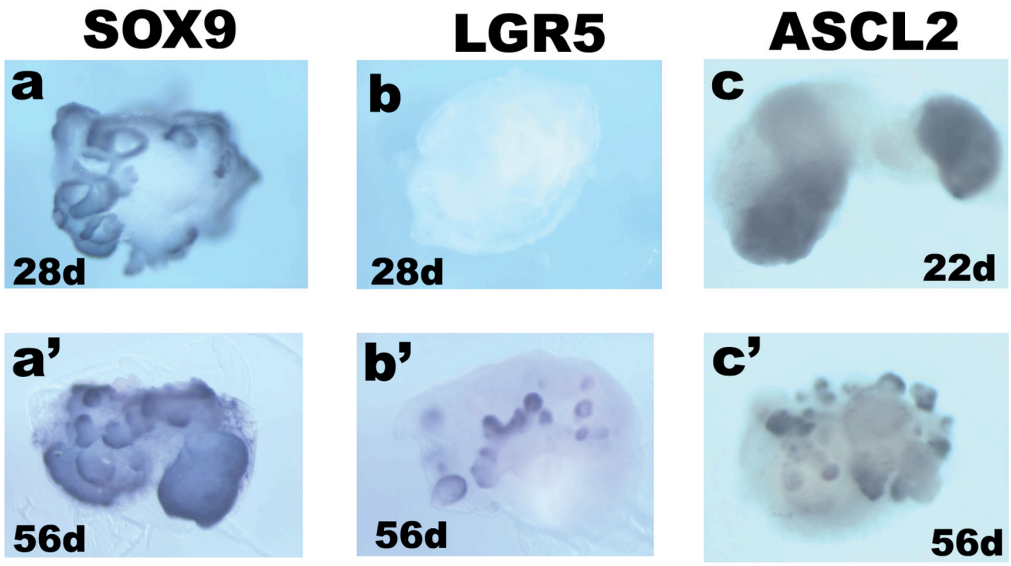

Supplementary Figure 10. Whole mount *in situ* hybridization (WMISH) for intestinal stem cell markers at different stages.
a and a', WMISH for SOX9 at 28 days (a) and 56 days (a') shows expression in peripheral regions of the epithelium that were adjacent to the mesenchyme. **b and b',** WMISH for LGR5 at 28 days (a) and 56 days (b) demonstrates undetectable levels of LGR5 at 28 days and *de novo* expression at 56 days in discrete "crypt-like" domains. **c and c',** WMISH for ASCL2 demonstrates weak, broad and weak expression at 22 days (c). At 56 days high levels of ASCL2 expression are restricted to discrete "crypt-like" domains (c') that correlate with the domains of LGR5 (b') and SOX9 expression (a').

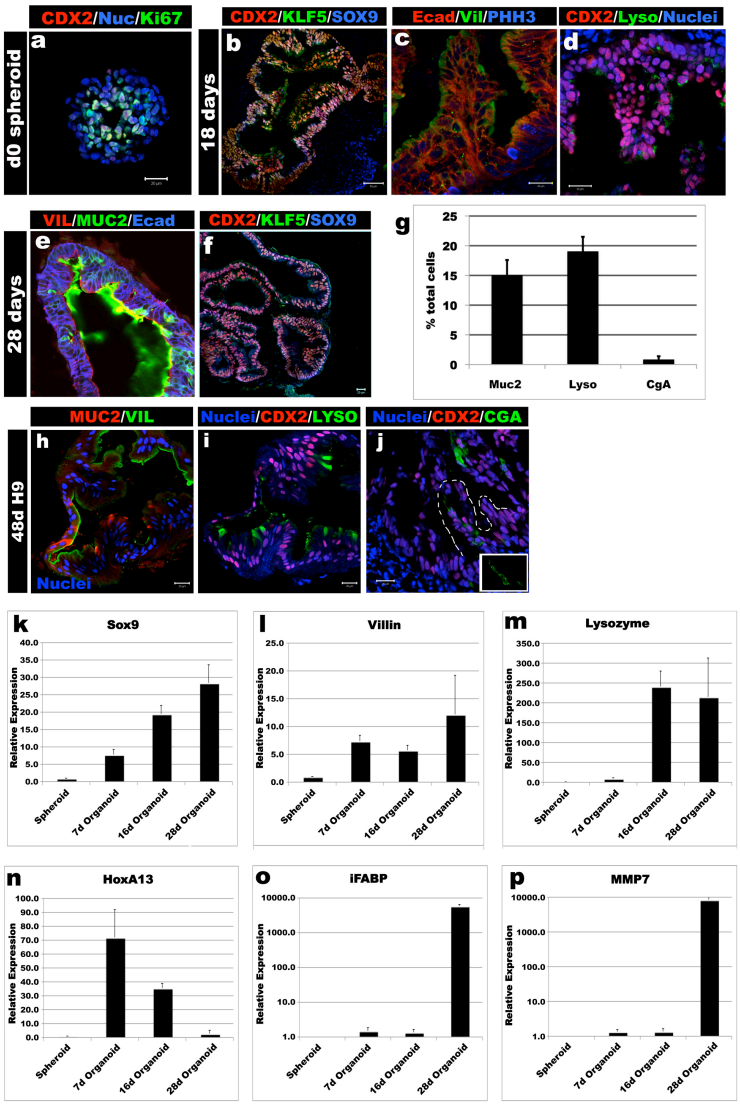

Supplementary Figure 11. Molecular analysis of stages of intestinal epithelial growth, maturation and cytodifferentiation in organoids.

a, 96 hours after FGF4+Wnt3a exposure, hindgut spheroids contained a highly proliferative cuboidal epithelium that expressed CDX2. **b-d,** 18 day iPSC-derived organoids contained a pseudostratified epithelium that broadly expressed CDX2, KLF5 and SOX9 (**b**), had weak apical Villin staining (**c**), and had begun expressing markers of cytodifferentiation including lysozyme (Lyso) (**d**). **e and f,** At 28 days, organoids secreted mucins into the lumen (**e - green**), broadly expressed CDX2 and KLF5 and showed restricted expression of SOX9 (**f**). **h-j,** 48 day hESC-derived organoids were analyzed for villin (VIL) and the goblet cell marker mucin (MUC2), **h,** the paneth cell marker lysozyme (LYSO), **i,** or the endocrine cell marker chromogranin A (CGA), **j**. **k-p,** Quantitative RT-QPCR analysis of intestinal markers SOX9, Villin (enterocytes), Lysozyme (Paneth cells), HOXA13, IFABP (enterocytes) and MMP7 (Paneth cells) during intestinal organoid development by RT-qPCR. Error bars S.E.M. (n=3 for each stage).

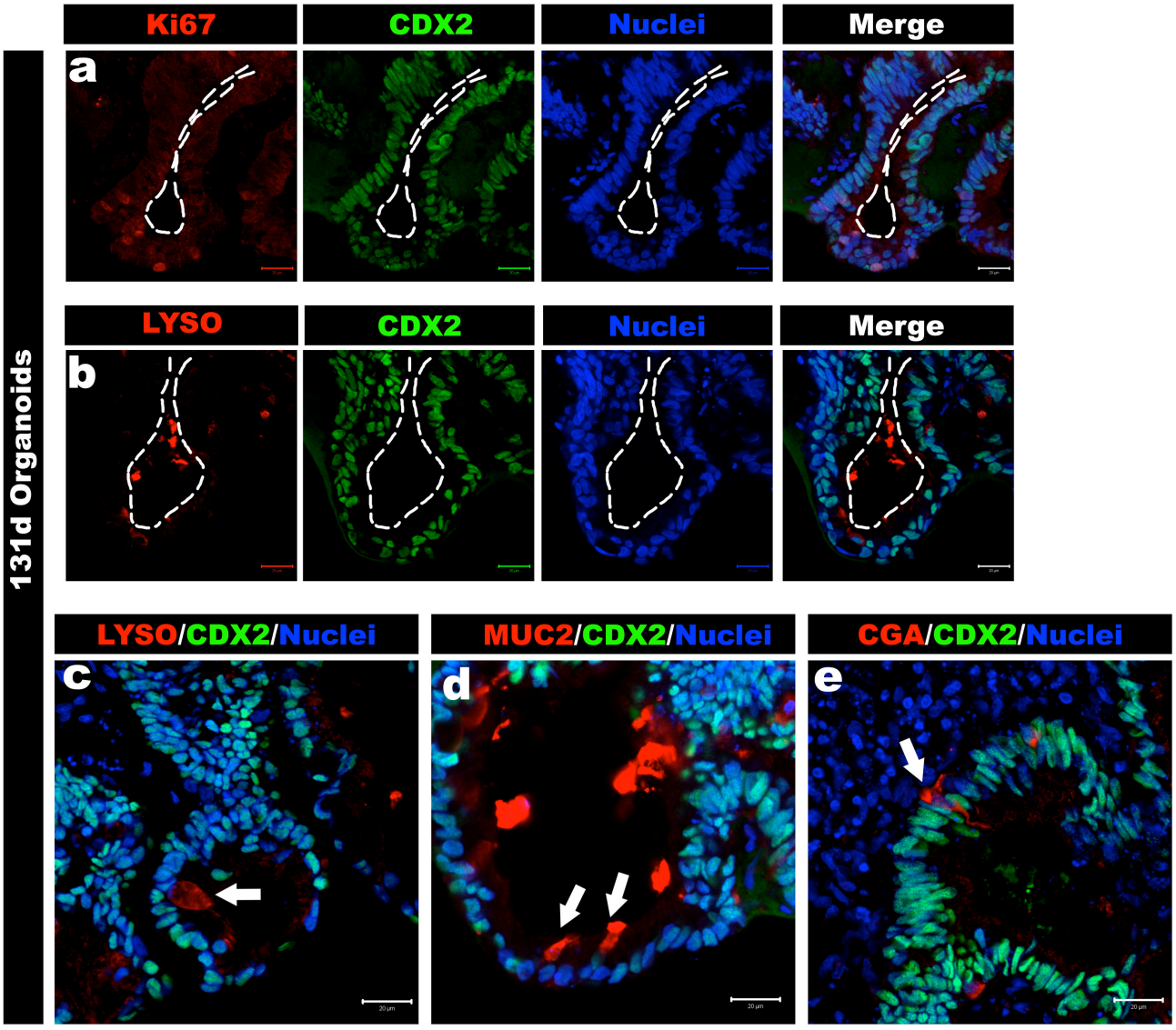

Supplementary Figure 12. Extended culturing allows for maturation of intestinal organoids. **a,** Ki67 staining (red) shows that proliferation was restricted to proliferative "crypt-like" domains that were present in 131-day old organoids. **b,** Serial section of (a) showing that the crypt-like domains also contained Lysozyme positive cells. **c, d and e,** Secretory cell types appeared more mature in 131-day old organoids, including **c,** Paneth cells (Lysozyme, red), **d,** goblet cells (MUC2, red) and **e,** enteroendocrine cells (ChromograninA, red).

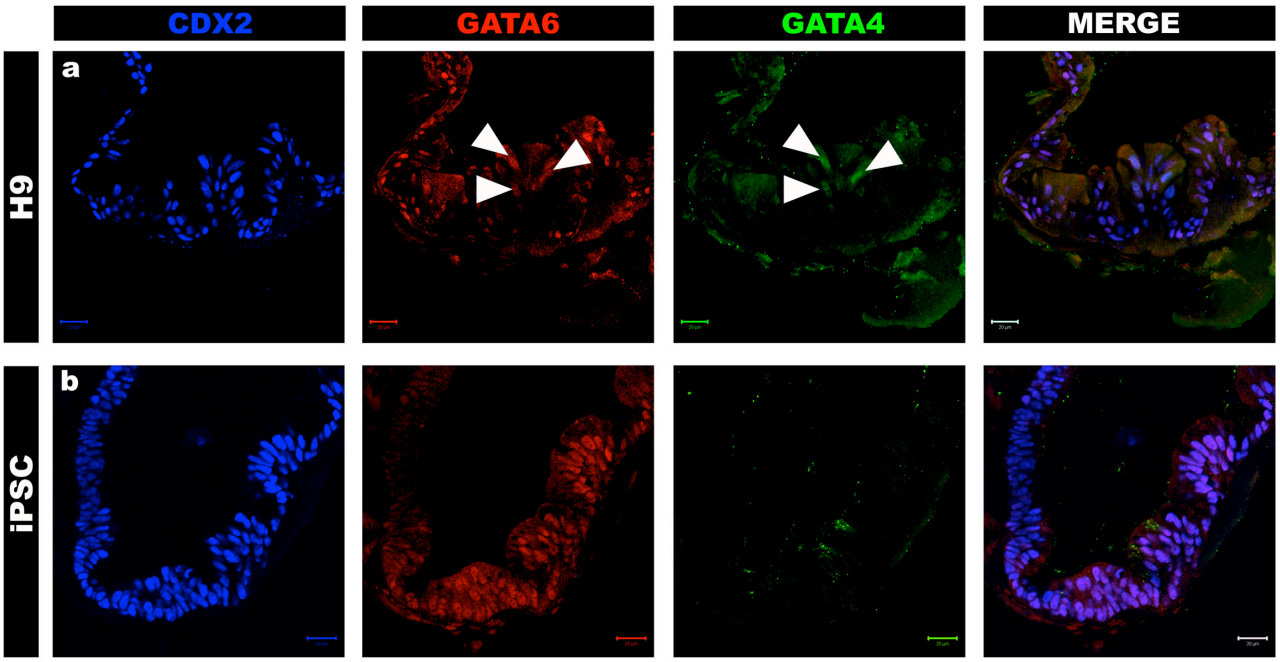

Supplementary Figure 13. GATA factor expression in organoids.
a, H9 hESC derived organoids show that most CDX2 (blue) positive nuclei express GATA6 (red), whereas only a few nuclei express GATA4 (green, white arrowheads). GATA4/6 double positive cells (white arrowheads) are indicative of proximal intestine, where as GATA6+/GATA4- cells are indicative of distal intestine. **b,** human iPSC derived organoids show that almost all CDX2 positive cells (blue) are GATA6 positive (red). In this example, the organoid did not express GATA4 (green) in this section of tissue, indicating that this intestinal tissue is distal intestine.

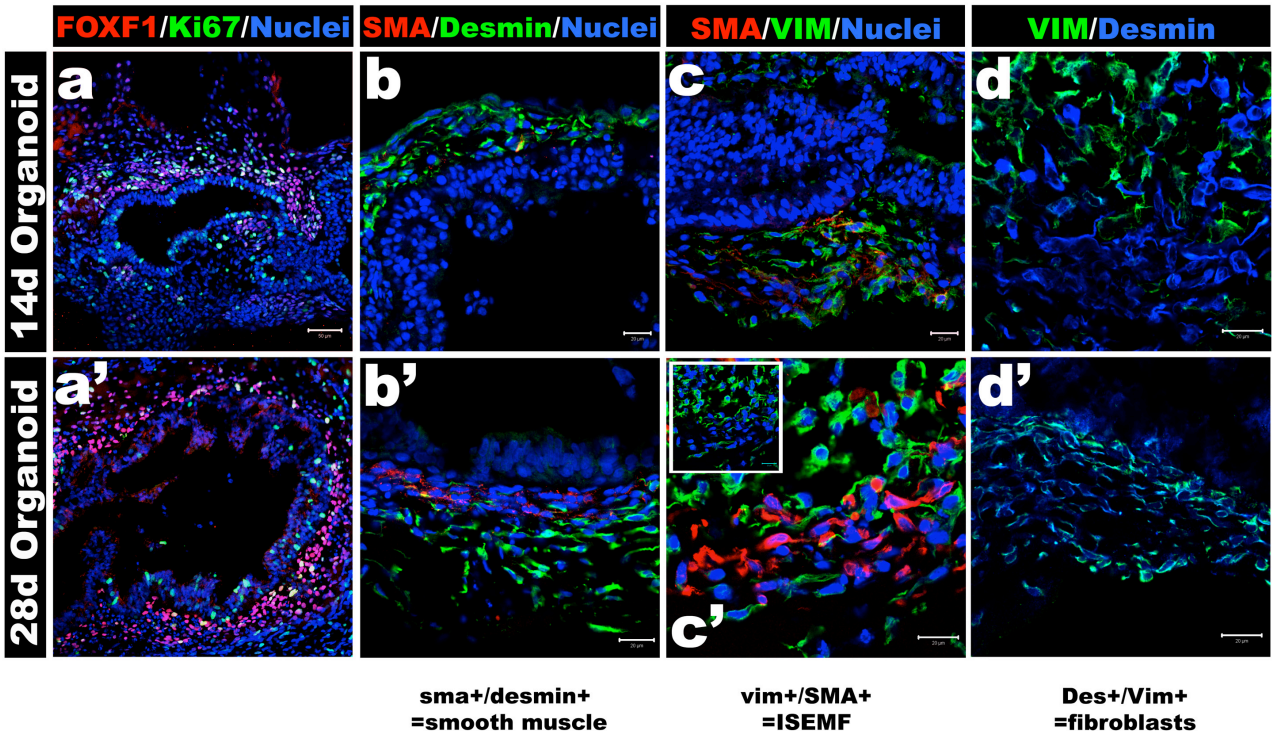

Supplementary Figure 14. Mesenchymal development and maturation in intestinal organoids. **a and a',** The marker FoxF1 (red) was expressed in the mesenchyme adjacent to intestinal epithelium in 14 day (a) and 28 day organoids (a'). Proliferation was shown by Ki67 staining (green). Nuclei are blue. **b and b',** SMA and Desmin co-staining indicates smooth muscle cells (SMA+/Desmin+). In 14 day organoids very few SMA+ (red) cells were seen and the majority of mesenchymal cells were desmin+ (green) (b). In contrast, more SMA+ cells were detected in 28d organoids, however, not all SMA+ cells were co-stained with desmin (yellow) (b'). **c and c',** SMA (red) and Vimentin (green) co-staining demonstrates intestinal subepithelial myofibroblasts (IMSEFs, SMA+/Vim+). Mesenchyme in 14 day organoids was mostly SMA+/Vim+, suggesting that these were undifferentiated IMSEFs (c) whereas at 28 days cells appeared to differentiate into different mesenchymal populations (c'). Inset in (c') shows Vimentin staining only (green). **d and d',** Vimentin (green) and Desmin (blue) co-staining suggests immature intestinal fibroblasts in both 14 day (d) and 28 day (d') organoids.

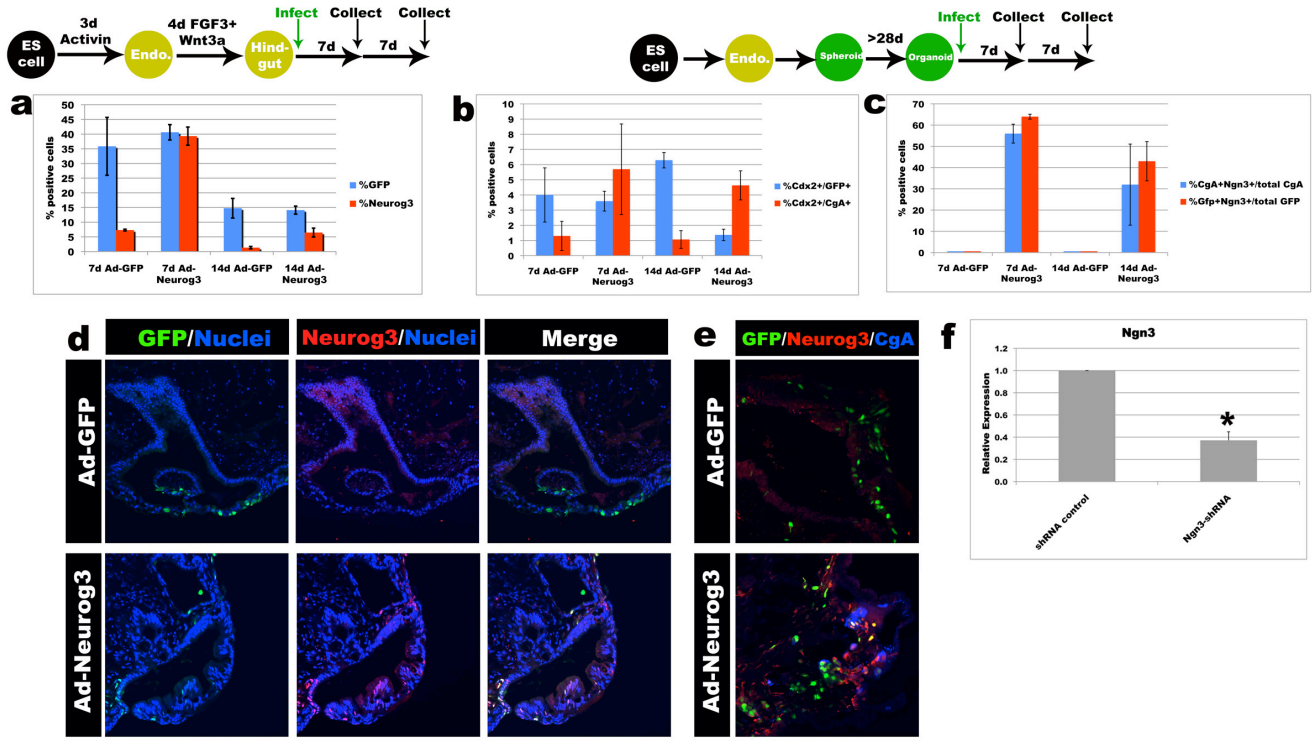

Supplementary Figure 15. Quantification of NEUROG3 over expression and siRNA knock down. **a,** Schematic of the experiment (top) shows a time course analysis of the total percent of cells infected in hindgut monolayers using control GFP adenovirus (Ad-GFP) or NEUROG3 adenovirus (Ad-NEUROG3). Analysis after 7 and 14 days of infection demonstrates the transient nature of Adenoviral infection over time. After 7 days, 35.8% of total cells in control and 40.6% of cells in Ad-NEUROG3 infected cultures showed GFP expression and 39.3% of cells expressed NEUROG3. After 14 days approximately 14% of cells were infected as measured by GFP expression (14.7% Ad-GFP, 14.1% Ad-NEUROG3) and adenoviral-NEUROG3 expression was decreased to 6.5%. **b and c,** Schematic of the experiment (top) where hESC derived intestinal organoids were infected for 8 hours with Ad-GFP control or Ad-NEUROG3 adenovirus and re-cultured for an additional 7 or 14 days. GFP expression showed that in contrast to monolayer cultures, only ~4% of organoid intestinal epithelial cells are infected with Adenovirus after 7 days (b). At both 7 and 14 days, the percent of epithelial cells that were co-labeled with the enteroendocrine marker CgA was increased in Ad-NEUROG3 compared to controls by ~5 fold (b). Many of the CgA+ cells also co-expressed NEUROG3 (56% and 32% of CgA+ cells co-expressed NEUROG3 after 7 and 14 days respectively (c)), suggesting that down regulation of endogenous NEUROG3 is coincident with differentiation of enteroendocrine cells but that down regulation is not required for differentiation to proceed. NEUROG3 expression in CgA+ was from the viral vector since these cells also expressed GFP. **d,** Representative images of intestinal organoids infected with Ad-GFP or Ad-NEUROG3 and immunostained for GFP (green), NEUROG3 (red) and counterstained with Draq5 (blue, nuclei). **e,** Intestinal organoids infected with Ad-GFP or Ad-NEUROG3 and immunostained for GFP (green), NEUROG3 (red) and CgA (blue). Numerous NEUROG3-expressing cells co-expressed CgA. **f,** qRT-PCR analysis of 28 day intestinal organoids generated from control shRNA or NEUROG3-shRNA H9 hESC cell lines showed a 63% reduction in NEUROG3 mRNA ($p=0.0012$). All error bars are S.E.M. and $n>=3$ for each experiment.

SUPPLEMENTARY TABLES

Supplementary Table 1a. Transcripts elevated two-fold or more during DE formation in HESC-H9 and iPSC lines 3.12 and 3.5.

Gene symbol	Fold change Diff. H9 vs Undiff. H9	Fold change Diff. iPSC3.12 vs Undiff. iPSC3.12	Fold change Diff. iPSC3.4 vs Undiff. iPSC3.4	Gene description
CER1	137.61	67.98	66.76	cerberus 1, cysteine knot superfamily, homolog (Xenopus laevis)
HAS2	32.29	15.27	13.43	hyaluronan synthase 2
PRDM1	30.35	24.92	21.56	PR domain containing 1, with ZNF domain
SEMA3E	30.17	21.66	19.36	sema domain, immunoglobulin domain (Ig), short basic domain, secreted, (semaphorin) 3E
MFAP4	28.35	29.08	35.47	microfibrillar-associated protein 4
EOMES	28.31	19.85	27.72	eomesodermin homolog (Xenopus laevis)
CYP26A1	28.12	41.18	47.21	cytochrome P450, family 26, subfamily A, polypeptide 1
SLC40A1	27.82	33.13	34.77	solute carrier family 40 (iron-regulated transporter), member 1
CXCR4	24.73	23.19	19.91	chemokine (C-X-C motif) receptor 4
FGF17	17.92	15.78	19.00	fibroblast growth factor 17
TRPA1	17.40	25.46	23.50	transient receptor potential cation channel, subfamily A, member 1
ANKRD1	17.20	11.45	8.97	ankyrin repeat domain 1 (cardiac muscle)
LOC100132916	15.91	12.59	9.65	similar to hCG1811192
PCDH10	15.88	18.81	23.07	protocadherin 10
RHOBTB3	15.76	12.01	8.61	Rho-related BTB domain containing 3
LGR5	15.44	12.18	12.88	leucine-rich repeat-containing G protein-coupled receptor 5
CD48	14.69	18.02	15.22	
ST8SIA4	14.68	10.83	9.75	ST8 alpha-N-acetyl-neuraminide alpha-2,8-sialyltransferase 4
COL5A2	14.57	13.25	15.28	collagen, type V, alpha 2
COLEC12	13.69	11.08	12.98	collectin sub-family member 12
FLRT3	12.96	15.64	11.19	fibronectin leucine rich transmembrane protein 3
CHL1	12.67	2.89	3.63	cell adhesion molecule with homology to L1CAM (close homolog of L1)
ELOVL2	12.67	6.73	6.61	elongation of very long chain fatty acids (FEN1/Elo2, SUR4/Elo3, yeast)-like 2
CCL2	12.64	18.30	14.69	chemokine (C-C motif) ligand 2
MIXL1	12.51	7.17	8.06	Mix1 homeobox-like 1 (Xenopus laevis)
MGST2	11.94	15.71	13.68	microsomal glutathione S-transferase 2
EHHADH	11.32	9.12	8.12	enoyl-Coenzyme A, hydratase/3-hydroxyacyl Coenzyme A dehydrogenase
PLXNA2	11.05	9.37	9.50	plexin A2
DIO3	10.97	9.31	7.22	deiodinase, iodothyronine, type III

KLF8	10.94	6.17	5.97	Kruppel-like factor 8
PEG10	10.92	3.35	3.97	paternally expressed 10
TDRD7	10.91	9.40	9.32	tudor domain containing 7
MANEA	10.90	8.67	8.97	mannosidase, endo-alpha
UPK1B	10.83	5.46	5.74	uroplakin 1B
ROR2	10.22	8.35	8.35	receptor tyrosine kinase-like orphan receptor 2
CCKBR	9.79	12.68	9.37	cholecystokinin B receptor
DKK1	9.66	6.27	7.27	dickkopf homolog 1 (Xenopus laevis)
SERPINB9	9.32	10.27	10.52	serpin peptidase inhibitor, clade B (ovalbumin), member 9
OR5P2	9.18	5.08	6.24	olfactory receptor, family 5, subfamily P, member 2
OVCH2	9.06	6.77	7.92	ovochymase 2
FRZB	8.79	5.92	5.20	frizzled-related protein
SAMD3	8.40	8.88	7.82	sterile alpha motif domain containing 3
HHEX	8.37	15.27	10.62	hematopoietically expressed homeobox
PPAPDC1A	8.00	4.50	3.94	phosphatidic acid phosphatase type 2 domain containing 1A
MYL7	7.96	6.41	7.32	myosin, light chain 7, regulatory
PLSCR4	7.87	7.11	8.62	phospholipid scramblase 4
ITGA5	7.82	4.31	4.38	integrin, alpha 5 (fibronectin receptor, alpha polypeptide)
ENC1	7.76	3.37	3.08	ectodermal-neural cortex (with BTB-like domain)
TNC	7.73	6.30	9.01	tenascin C (hexabrachion)
C5	7.59	14.18	14.56	complement component 5
SOX17	7.34	7.29	7.58	SRY (sex determining region Y)-box 17
RLBP1L2	7.31	6.87	6.65	retinaldehyde binding protein 1-like 2
VAMP8	7.30	3.74	4.09	vesicle-associated membrane protein 8 (endobrevin)
PLCE1	7.11	7.55	6.70	phospholipase C, epsilon 1
NTN4	7.09	6.11	5.15	netrin 4
PROS1	7.01	4.02	4.07	protein S (alpha)
LRIG3	6.97	9.55	9.18	leucine-rich repeats and immunoglobulin-like domains 3
CDH2	6.89	8.08	7.38	cadherin 2, type 1, N-cadherin (neuronal)
CFLAR	6.84	6.90	6.63	CASP8 and FADD-like apoptosis regulator
ARHGAP24	6.74	5.33	5.92	Rho GTPase activating protein 24
C6orf60	6.67	7.85	6.40	chromosome 6 open reading frame 60
MCC	6.48	3.48	3.37	mutated in colorectal cancers
GPR177	6.42	5.21	4.84	G protein-coupled receptor 177
CPE	6.36	7.33	6.89	carboxypeptidase E
C9orf19	6.14	5.15	5.52	chromosome 9 open reading frame 19
PLSCR1	5.99	4.35	3.70	phospholipid scramblase 1
BMP2	5.95	7.43	6.96	bone morphogenetic protein 2
OR5P3	5.80	3.50	4.65	olfactory receptor, family 5, subfamily P, member 3
FN1	5.77	3.80	3.73	fibronectin 1
TBC1D9	5.72	5.94	5.11	TBC1 domain family, member 9 (with GRAM domain)
VWF	5.69	5.27	5.12	von Willebrand factor
NODAL	5.66	5.77	5.00	nodal homolog (mouse)
GSC	5.57	5.37	5.22	goosecoid homeobox
SMAD6	5.53	2.54	2.97	SMAD family member 6
S100Z	5.52	4.68	4.36	S100 calcium binding protein Z
ARHGAP29	5.52	4.47	4.19	Rho GTPase activating protein 29

LHX1	5.51	4.72	4.60	LIM homeobox 1
ARSE	5.42	5.47	5.25	arylsulfatase E (chondrodysplasia punctata 1)
CNGA4	5.39	4.06	4.78	cyclic nucleotide gated channel alpha 4
AHNAK	5.34	4.93	4.71	
SEPP1	5.28	5.27	4.42	selenoprotein P, plasma, 1
PROS1	5.23	3.60	3.95	protein S (alpha)
CALCR	5.20	3.44	3.13	calcitonin receptor
IER3	5.14	6.06	5.38	immediate early response 3
MAN1A1	5.12	4.60	4.23	mannosidase, alpha, class 1A, member 1
KCNG1	5.09	3.70	4.11	potassium voltage-gated channel, subfamily G, member 1
BNIP3	5.08	3.56	3.35	BCL2/adenovirus E1B 19kDa interacting protein 3
H2AFY2	5.05	7.17	6.81	H2A histone family, member Y2
FAM122C	5.03	4.61	4.20	family with sequence similarity 122C
FMN2	5.03	3.77	4.77	formin 2
PPFIBP2	5.03	4.02	4.10	PTPRF interacting protein, binding protein 2 (liprin beta 2)
ARRDC3	4.99	4.14	3.33	arrestin domain containing 3
GATM	4.99	4.95	3.94	glycine amidinotransferase (L-arginine:glycine amidinotransferase)
C21orf129	4.97	10.33	8.83	chromosome 21 open reading frame 129
KRT8	4.96	2.41	2.50	keratin 8
ADAM19	4.96	4.37	4.36	ADAM metallopeptidase domain 19 (meltrin beta)
BTG2	4.90	3.29	3.20	BTG family, member 2
ARRB1	4.90	2.66	3.03	arrestin, beta 1
AGL	4.90	3.65	3.09	amylo-1, 6-glucosidase, 4-alpha-glucanotransferase (glycogen debranching enzyme, glycogen storage disease type III)
IFLTD1	4.86	2.44	2.79	intermediate filament tail domain containing 1
TIPARP	4.84	4.13	3.77	TCDD-inducible poly(ADP-ribose) polymerase
NFKBIA	4.83	4.56	4.41	nuclear factor of kappa light polypeptide gene enhancer in B-cells inhibitor, alpha
RNF19A	4.79	5.77	4.63	ring finger protein 19A
PDZK1	4.77	3.94	3.57	PDZ domain containing 1
RNF152	4.77	4.66	4.52	ring finger protein 152
RPRM	4.76	4.83	4.58	reprimo, TP53 dependent G2 arrest mediator candidate
TGFB1	4.74	2.98	3.54	transforming growth factor, beta 1
CAMK2D	4.64	4.00	3.77	calcium/calmodulin-dependent protein kinase (CaM kinase) II delta
ARL4D	4.62	4.07	3.95	ADP-ribosylation factor-like 4D
ARHGAP28	4.60	3.54	3.27	Rho GTPase activating protein 28
C8orf49	4.59	4.09	3.45	chromosome 8 open reading frame 49
MATN3	4.57	4.36	5.19	matrilin 3
DUSP10	4.54	4.45	4.76	dual specificity phosphatase 10
PTPRM	4.51	5.04	5.21	protein tyrosine phosphatase, receptor type, M
RNF125	4.49	3.53	3.28	ring finger protein 125
ACOX3	4.48	5.42	5.45	acyl-Coenzyme A oxidase 3, pristanoyl
SLC22A3	4.40	4.27	5.11	solute carrier family 22 (extraneuronal monoamine transporter), member 3
IER3	4.39	4.79	4.34	immediate early response 3

NR0B1	4.39	11.17	9.41	nuclear receptor subfamily 0, group B, member 1
S1PR3|C9orf 47	4.39	3.21	4.05	sphingosine-1-phosphate receptor 3 | chromosome 9 open reading frame 47
IER3	4.39	4.80	4.34	immediate early response 3
C8orf79	4.32	3.02	2.86	chromosome 8 open reading frame 79
EPSTI1	4.32	4.91	4.62	epithelial stromal interaction 1 (breast)
KRT19	4.27	2.48	2.56	keratin 19
USP53	4.26	3.53	3.00	ubiquitin specific peptidase 53
GPSM2	4.21	5.06	4.09	G-protein signaling modulator 2 (AGS3-like, C. elegans)
PRSS35	4.19	5.55	5.36	protease, serine, 35
RELN	4.13	3.02	3.30	reelin
RBM24	4.12	4.75	3.60	RNA binding motif protein 24
RASGEF1B	4.05	3.15	3.59	RasGEF domain family, member 1B
MERTK	4.01	3.13	3.67	c-mer proto-oncogene tyrosine kinase
OTX2	4.01	5.22	5.32	orthodenticle homeobox 2
MAML3	4.00	3.41	3.52	mastermind-like 3 (Drosophila)
PDE10A	3.98	4.60	4.58	phosphodiesterase 10A
PLCXD3	3.98	3.34	2.49	phosphatidylinositol-specific phospholipase C, X domain containing 3
GREM2	3.97	3.14	3.50	gremlin 2, cysteine knot superfamily, homolog (Xenopus laevis)
MYO3A	3.93	4.17	4.62	myosin IIIA
NEK7	3.92	3.53	3.02	NIMA (never in mitosis gene a)-related kinase 7
LEPREL1	3.92	6.42	6.24	leprecan-like 1
MOBP	3.92	2.68	2.52	myelin-associated oligodendrocyte basic protein
KCNH8	3.87	4.09	3.76	potassium voltage-gated channel, subfamily H (eag-related), member 8
FAM20A	3.84	4.69	5.21	family with sequence similarity 20, member A
MID2	3.83	2.46	2.43	midline 2
SETD7	3.82	3.65	3.68	SET domain containing (lysine methyltransferase) 7
MYCT1	3.79	6.63	6.07	myc target 1
KIAA0825	3.75	4.30	4.73	
FLRT2	3.74	2.88	3.40	fibronectin leucine rich transmembrane protein 2
PREX1	3.73	2.87	3.03	phosphatidylinositol 3,4,5-trisphosphate-dependent RAC exchanger 1
ASAM	3.73	3.68	3.58	adipocyte-specific adhesion molecule
CYP1B1	3.71	2.20	2.15	cytochrome P450, family 1, subfamily B, polypeptide 1
YPEL5	3.70	2.91	2.95	yippee-like 5 (Drosophila)
SEMA5A	3.69	5.53	5.37	sema domain, seven thrombospondin repeats (type 1 and type 1-like), transmembrane domain (TM) and short cytoplasmic domain, (semaphorin) 5A
LEFTY2	3.68	8.55	6.11	left-right determination factor 2
C9orf52	3.62	3.58	3.12	chromosome 9 open reading frame 52
SLITRK2|LO C100129095	3.62	3.66	3.73	SLIT and NTRK-like family, member 2 | similar to CXorf2 protein
SERPINE2	3.61	3.78	3.80	serpin peptidase inhibitor, clade E (nexin, plasminogen activator inhibitor type 1), member 2
B3GNT5	3.57	2.85	2.91	UDP-GlcNAc:betaGal beta-1,3-N-acetylglucosaminyltransferase 5

SLCO2A1	3.57	2.32	2.14	solute carrier organic anion transporter family, member 2A1
SLC35F3	3.55	3.21	3.38	solute carrier family 35, member F3
SOX5	3.55	4.09	3.99	SRY (sex determining region Y)-box 5
NUDT4P1	3.54	2.88	2.42	nudix (nucleoside diphosphate linked moiety X)-type motif 4 pseudogene 1
ANGPT2	3.54	5.23	3.90	angiopoietin 2
CAP2	3.53	2.97	3.00	CAP, adenylate cyclase-associated protein, 2 (yeast)
NETO2	3.50	2.25	2.21	neuropilin (NRP) and tolloid (TLL)-like 2
TRY6|PRSS2|PRSS1|PRSS3|LOC100134294	3.50	3.12	3.59	trypsinogen C | protease, serine, 2 (trypsin 2) | protease, serine, 1 (trypsin 1) | protease, serine, 3 | hypothetical protein LOC100134294
ANGPT1	3.49	3.56	3.37	angiopoietin 1
VANGL1	3.48	2.94	2.79	vang-like 1 (van gogh, Drosophila)
CDA	3.48	4.14	3.63	cytidine deaminase
MCF2L2	3.46	3.33	3.11	MCF.2 cell line derived transforming sequence-like 2
C9orf95	3.44	2.28	2.13	chromosome 9 open reading frame 95
GATA4	3.42	2.89	2.77	GATA binding protein 4
MAGI3	3.39	3.20	3.13	membrane associated guanylate kinase, WW and PDZ domain containing 3
WNT3	3.39	2.97	3.36	wingless-type MMTV integration site family, member 3
APOBEC3G|APOBEC3F	3.36	2.79	2.90	apolipoprotein B mRNA editing enzyme, catalytic polypeptide-like 3G | apolipoprotein B mRNA editing enzyme, catalytic polypeptide-like 3F
FOXA2	3.36	3.08	3.93	forkhead box A2
BRDT	3.34	2.82	2.33	bromodomain, testis-specific
tcag7.1177	3.33	2.60	3.10	opposite strand transcription unit to STAG3
LOC389523|LOC729438|LOC730322	3.33	2.59	3.10	similar to opposite strand transcription unit to Stag3
ZSWIM5	3.32	2.79	2.75	zinc finger, SWIM-type containing 5
COCH	3.32	2.08	2.53	coagulation factor C homolog, cochlin (Limulus polyphemus)
EPHA4	3.31	4.54	4.66	EPH receptor A4
C1orf61	3.30	3.51	3.49	chromosome 1 open reading frame 61
KEL	3.29	4.02	4.07	Kell blood group, metallo-endopeptidase
PPM1K	3.29	3.71	3.74	protein phosphatase 1K (PP2C domain containing)
SORCS1	3.29	3.64	4.01	sortilin-related VPS10 domain containing receptor 1
SLC46A3	3.28	2.01	2.00	solute carrier family 46, member 3
BHLHB2	3.23	2.26	2.43	basic helix-loop-helix domain containing, class B, 2
BMPR2	3.23	3.64	3.57	bone morphogenetic protein receptor, type II (serine/threonine kinase)
CAMKK2	3.21	2.94	3.14	calcium/calmodulin-dependent protein kinase kinase 2, beta
DAB2	3.21	2.38	2.30	disabled homolog 2, mitogen-responsive phosphoprotein (Drosophila)
ELMO1	3.20	5.68	4.76	engulfment and cell motility 1
SEMA6D	3.20	6.82	6.05	sema domain, transmembrane domain (TM), and

				cytoplasmic domain, (semaphorin) 6D
CXCR7	3.20	3.18	3.21	chemokine (C-X-C motif) receptor 7
P4HA1	3.20	2.63	2.45	procollagen-proline, 2-oxoglutarate 4-dioxygenase (proline 4-hydroxylase), alpha polypeptide I
YAF2	3.17	2.48	2.87	YY1 associated factor 2
TMOD1	3.16	2.61	2.62	tropomodulin 1
RALB	3.16	2.41	2.11	v-ral simian leukemia viral oncogene homolog B (ras related; GTP binding protein)
FBN2	3.13	3.58	4.30	fibrillin 2 (congenital contractural arachnodactyly)
KIAA1161	3.10	2.84	3.74	
LTB4DH	3.10	3.08	2.77	leukotriene B4 12-hydroxydehydrogenase
DUSP4	3.10	3.14	2.43	dual specificity phosphatase 4
GPR39	3.09	5.74	6.56	G protein-coupled receptor 39
CNTN4	3.08	2.58	2.54	contactin 4
FRRS1	3.06	2.21	2.07	ferric-chelate reductase 1
PGM1	3.03	2.67	2.67	phosphoglucomutase 1
PDK1	3.03	4.84	5.36	pyruvate dehydrogenase kinase, isozyme 1
SOAT1	3.03	3.19	2.88	sterol O-acyltransferase (acyl-Coenzyme A: cholesterol acyltransferase) 1
CCDC92	3.00	2.79	2.97	coiled-coil domain containing 92
ZNF792	3.00	2.44	2.22	zinc finger protein 792
SLC35A3	3.00	3.55	2.83	solute carrier family 35 (UDP-N-acetylglucosamine (UDP-GlcNAc) transporter), member A3
SMAD7	3.00	2.23	2.07	SMAD family member 7
CEP55	2.99	2.02	2.08	centrosomal protein 55kDa
DDAH2	2.99	2.14	2.44	dimethylarginine dimethylaminohydrolase 2
DDAH2	2.98	2.15	2.44	dimethylarginine dimethylaminohydrolase 2
APOC1	2.97	2.73	2.14	apolipoprotein C-I
TMEM133	2.95	3.63	3.12	transmembrane protein 133
HNF1B	2.95	2.25	2.64	HNF1 homeobox B
FLJ32810	2.94	3.55	2.92	
RAP1GDS1	2.91	2.27	2.38	RAP1, GTP-GDP dissociation stimulator 1
DDAH2	2.90	2.08	2.29	dimethylarginine dimethylaminohydrolase 2
C5orf36	2.90	2.59	2.45	chromosome 5 open reading frame 36
GCNT1	2.89	4.78	5.38	glucosaminyl (N-acetyl) transferase 1, core 2 (beta-1,6-N-acetylglucosaminyltransferase)
APOBEC3D	2.89	2.21	2.03	apolipoprotein B mRNA editing enzyme, catalytic polypeptide-like 3D
NPPB	2.88	3.62	3.57	natriuretic peptide precursor B
MLYCD	2.87	2.89	2.78	malonyl-CoA decarboxylase
AADAT	2.86	2.49	2.25	aminoadipate aminotransferase
STMN2	2.85	5.88	5.04	stathmin-like 2
SULF2	2.85	3.19	2.99	sulfatase 2
ANKRD6	2.84	3.01	3.06	ankyrin repeat domain 6
TBX3	2.84	2.18	2.16	T-box 3 (ulnar mammary syndrome)
APOA2	2.83	3.62	3.42	apolipoprotein A-II
PPFIBP1	2.83	2.60	2.45	PTPRF interacting protein, binding protein 1 (liprin beta 1)
ALDH1A1	2.82	2.46	2.18	aldehyde dehydrogenase 1 family, member A1
LIFR	2.82	2.31	2.51	leukemia inhibitory factor receptor alpha

ID1	2.81	2.49	2.73	inhibitor of DNA binding 1, dominant negative helix-loop-helix protein
MTUS1	2.81	2.72	2.99	mitochondrial tumor suppressor 1
MYL4	2.80	2.45	2.05	myosin, light chain 4, alkali; atrial, embryonic
YPEL2	2.80	2.68	2.30	yippee-like 2 (Drosophila)
FZD5	2.80	6.24	5.60	frizzled homolog 5 (Drosophila)
TNNC1	2.80	2.31	2.03	troponin C type 1 (slow)
TMPRSS11E |TMPRSS11 E2	2.79	3.23	3.04	transmembrane protease, serine 11E | transmembrane protease, serine 11E2
CCDC75	2.78	2.47	2.15	coiled-coil domain containing 75
EGF	2.78	4.20	3.94	epidermal growth factor (beta-urogastrone)
KIT	2.78	4.03	3.60	v-kit Hardy-Zuckerman 4 feline sarcoma viral oncogene homolog
TMPRSS11E |TMPRSS11 E2	2.76	3.23	2.97	transmembrane protease, serine 11E | transmembrane protease, serine 11E2
KCNG1	2.72	2.33	2.68	potassium voltage-gated channel, subfamily G, member 1
CUGBP2	2.72	2.54	2.11	CUG triplet repeat, RNA binding protein 2
CDH10	2.71	3.23	4.02	cadherin 10, type 2 (T2-cadherin)
LEFTY1	2.70	4.86	5.04	left-right determination factor 1
C20orf95	2.68	3.26	3.35	chromosome 20 open reading frame 95
ACSS3	2.67	2.12	2.10	acyl-CoA synthetase short-chain family member 3
FAM126B	2.67	2.27	2.00	family with sequence similarity 126, member B
PERP	2.66	2.40	2.73	
GATA6	2.65	3.93	4.05	GATA binding protein 6
ANKS1B	2.64	2.39	2.26	ankyrin repeat and sterile alpha motif domain containing 1B
CA2	2.61	2.48	2.36	carbonic anhydrase II
TMEM135	2.58	2.71	2.72	transmembrane protein 135
CCDC3	2.58	2.68	2.84	coiled-coil domain containing 3
JAKMIP1	2.57	2.02	2.07	janus kinase and microtubule interacting protein 1
APOBEC3C| APOBEC3D	2.55	2.40	2.44	apolipoprotein B mRNA editing enzyme, catalytic polypeptide-like 3C | apolipoprotein B mRNA editing enzyme, catalytic polypeptide-like 3D
FZD8	2.54	3.57	3.26	frizzled homolog 8 (Drosophila)
SYNJ1	2.54	2.43	2.33	synaptojanin 1
GATA3	2.54	2.04	2.15	GATA binding protein 3
QPCT	2.53	3.59	3.29	glutaminyl-peptide cyclotransferase (glutaminyl cyclase)
C8orf79	2.52	2.17	2.90	chromosome 8 open reading frame 79
ZNF702	2.52	2.41	2.01	zinc finger protein 702
EDNRA	2.52	2.69	2.27	endothelin receptor type A
MAGED1	2.51	2.89	2.99	melanoma antigen family D, 1
DTWD2	2.50	2.53	2.32	DTW domain containing 2
KITLG	2.48	2.12	2.82	KIT ligand
APOBEC3F| APOBEC3G	2.48	2.48	2.29	apolipoprotein B mRNA editing enzyme, catalytic polypeptide-like 3F | apolipoprotein B mRNA editing enzyme, catalytic polypeptide-like 3G
ETS2	2.47	2.17	2.05	v-ets erythroblastosis virus E26 oncogene homolog 2

				(avian)
GNAL	2.46	3.70	3.72	guanine nucleotide binding protein (G protein), alpha activating activity polypeptide, olfactory type
ZNF518B	2.45	3.00	2.39	zinc finger protein 518B
HGSNAT	2.45	2.95	2.90	heparan-alpha-glucosaminide N-acetyltransferase
B4GALT4	2.42	2.12	2.05	UDP-Gal:betaGlcNAc beta 1,4- galactosyltransferase, polypeptide 4
ATP8A1	2.42	2.91	2.77	ATPase, aminophospholipid transporter (APLT), class I, type 8A, member 1
SYT10	2.41	2.13	2.26	synaptotagmin X
EFNA5	2.41	2.62	2.83	ephrin-A5
SMARCD3	2.40	2.70	2.39	SWI/SNF related, matrix associated, actin dependent regulator of chromatin, subfamily d, member 3
WDR44	2.40	2.48	2.26	WD repeat domain 44
EPHA2	2.39	2.03	2.12	EPH receptor A2
BCAR3	2.38	2.41	2.31	breast cancer anti-estrogen resistance 3
UNC50	2.36	3.44	3.34	unc-50 homolog (C. elegans)
LY6E	2.36	2.35	2.14	lymphocyte antigen 6 complex, locus E
SLC5A9	2.34	7.86	6.18	solute carrier family 5 (sodium/glucose cotransporter), member 9
COL4A1	2.33	2.20	2.15	collagen, type IV, alpha 1
KIAA0825	2.32	2.72	2.49	
NSUN3	2.32	2.41	2.15	NOL1/NOP2/Sun domain family, member 3
HEBP2	2.32	2.58	2.45	heme binding protein 2
COL6A1	2.32	2.20	2.52	collagen, type VI, alpha 1
PMEPA1	2.31	2.35	2.24	prostate transmembrane protein, androgen induced 1
STC1	2.30	2.94	3.30	stanniocalcin 1
MBNL3	2.29	2.65	2.47	muscleblind-like 3 (Drosophila)
FST	2.29	2.59	2.99	follistatin
TNRC18|LOC27320	2.28	2.09	2.17	trinucleotide repeat containing 18 | hypothetical protein LOC27320
LRRC3	2.25	2.18	2.53	leucine rich repeat containing 3
INPP4A	2.25	2.50	2.55	inositol polyphosphate-4-phosphatase, type I, 107kDa
RRAGB	2.25	2.26	2.21	Ras-related GTP binding B
SLC9A9	2.25	2.70	3.10	solute carrier family 9 (sodium/hydrogen exchanger), member 9
TMEM123	2.25	2.26	2.27	transmembrane protein 123
GPR151	2.24	5.25	4.07	G protein-coupled receptor 151
NR3C1	2.24	2.58	2.64	nuclear receptor subfamily 3, group C, member 1 (glucocorticoid receptor)
FAM89A	2.22	2.14	2.32	family with sequence similarity 89, member A
SHISA3	2.21	3.03	2.52	shisa homolog 3 (Xenopus laevis)
GLT1D1	2.21	2.71	2.37	glycosyltransferase 1 domain containing 1
NRIP1	2.21	2.18	2.02	nuclear receptor interacting protein 1
WNT8A	2.21	3.19	2.99	wingless-type MMTV integration site family, member 8A
AKAP13	2.20	2.05	2.08	A kinase (PRKA) anchor protein 13
GPR37	2.20	2.36	2.53	G protein-coupled receptor 37 (endothelin receptor type B-like)
COL4A6	2.19	2.76	3.25	collagen, type IV, alpha 6

DMN	2.19	2.05	2.34	desmuslin
PHF10	2.17	2.02	2.05	PHD finger protein 10
CCDC46	2.17	2.06	2.09	coiled-coil domain containing 46
TBX20	2.15	2.06	2.21	T-box 20
RCAN3	2.15	2.42	2.48	RCAN family member 3
ATP2B4	2.15	2.96	2.97	ATPase, Ca++ transporting, plasma membrane 4
FBXO34	2.15	2.05	2.19	F-box protein 34
C1orf97	2.15	2.13	2.08	chromosome 1 open reading frame 97
MAPK10	2.14	2.59	2.41	mitogen-activated protein kinase 10
CCNG2	2.13	2.17	2.08	cyclin G2
CYP27A1	2.12	3.89	3.49	cytochrome P450, family 27, subfamily A, polypeptide 1
FUT8	2.12	3.09	2.80	fucosyltransferase 8 (alpha (1,6) fucosyltransferase)
CTBS	2.11	2.58	2.41	chitobiase, di-N-acetyl-
ODZ4	2.10	2.46	2.76	odz, odd Oz/ten-m homolog 4 (Drosophila)
TRAF5	2.10	2.09	2.02	TNF receptor-associated factor 5
FZD4	2.09	2.40	2.63	frizzled homolog 4 (Drosophila)
PCDH7	2.09	3.85	4.19	protocadherin 7
IL18R1	2.09	2.89	2.88	interleukin 18 receptor 1
PLXNA4	2.06	2.09	2.27	plexin A4
KCNK12	2.06	2.44	2.20	potassium channel, subfamily K, member 12
GPM6A	2.04	5.17	5.20	glycoprotein M6A
MAGED2	2.04	2.12	2.28	melanoma antigen family D, 2
PDGFC	2.04	2.14	2.30	platelet derived growth factor C
IFI16	2.03	4.18	3.33	interferon, gamma-inducible protein 16
ABCC4	2.03	3.31	2.93	ATP-binding cassette, sub-family C (CFTR/MRP), member 4
C4orf35	2.02	2.19	2.01	chromosome 4 open reading frame 35
ELMOD2	2.01	2.42	2.07	ELMO/CED-12 domain containing 2
SH3RF1	2.01	2.35	2.34	SH3 domain containing ring finger 1

Supplementary Table 1b. Transcripts elevated in both HESC-DE and DE dissected from e7.5 mouse embryos.

Symbol	Gene name	Reference
ADAM19	ADAM metallopeptidase domain 19 (meltrin beta)	
APOA1	apolipoprotein A-I	
APOE	apolipoprotein E	
BAMBI	BMP and activin membrane-bound inhibitor homolog	[39]
BMP2	bone morphogenetic protein 2	[40]
BMP7	bone morphogenetic protein 7 (osteogenic protein 1)	[41]
CDKN1C	Cyclin-dependent kinase inhibitor 1C (p57, Kip2)	
CER1	cerberus 1, cysteine knot superfamily, homolog	
COL5A2	collagen, type V, alpha 2	
COL4A5	collagen, type IV, alpha 5 (Alport syndrome)	
COL9A2	collagen, type IX, alpha 2	
CRIP1	cysteine-rich protein 1 (intestinal) /// galactokinase 2	

CXCR4	chemokine (C-X-C motif) receptor 4	
DAB2	disabled homolog 2, mitogen-responsive phosphoprotein	
DKK1	dickkopf homolog 1 (Xenopus laevis)	
DKK3	dickkopf homolog 3 (Xenopus laevis)	
EOMES	eomesodermin homolog	
EPHA2	EPH receptor A2	
ESRRG	estrogen-related receptor gamma (alpha in mouse)	
EYA1	eyes absent homolog 1 (Drosophila) Eya2 mouse	[42]
FKBP9	FK506 binding protein 9, 63 kDa	
FOXA1	forkhead box A1	
FOXA2	forkhead box A2	
FOXC1	forkhead box C1 (Foxc2 in mouse)	
FZD4	frizzled homolog 4 (Drosophila)	
GAD1	glutamate decarboxylase 1 (brain, 67kDa) (Glud in mouse)	
GATA3	GATA binding protein 3	
GATA4	GATA binding protein 4	[43]
GATA6	GATA binding protein 6	[43]
GLIS3	GLIS family zinc finger 3	
GLUD1	glutamate dehydrogenase 1	
GLUD2	glutamate dehydrogenase 2	
GSC	goosecoid homeobox	[44]
H2AFY2	H2A histone family, member Y2	
HHEX	homeobox, hematopoietically expressed	[45]
HSZFP36	ZFP-36 for a zinc finger protein	
ID1	inhibitor of DNA binding 1, dominant negative helix-loop-helix protein	
ID3	inhibitor of DNA binding 3, dominant negative helix-loop-helix protein	
IGF2	insulin-like growth factor 2	
IGFBP3	insulin-like growth factor binding protein 3	
KIT	v-kit Hardy-Zuckerman 4 feline sarcoma viral oncogene homolog	
KRT19	keratin 19	
KRT8	keratin 8 /// keratin 8 (alias Endo A mouse)	
LEFTY1	left-right determination factor 1	[46,47]
LEFTY2	left-right determination factor 2	[48]
LHX1	LIM homeobox 1	
MANEA	mannosidase, endo-alpha	
MANEAL	mannosidase, endo-alpha-like	
MIXL1	Mix1 homeobox-like 1	[49]
MSX2	msh homeobox homolog 2 (Drosophila) (Msx1 mouse)	
NID2	nidogen 2 (osteonidogen)	
NODAL	nodal homolog	
NRP1	neuropilin 1	
OTX2	orthodenticle homeobox 2	[50]
PDZK1	PDZ domain containing 1	
PERP	PERP, TP53 apoptosis effector	
PPOX	protoporphyrinogen oxidase	

SOX17	SRY (sex determining region Y)-box 17	
SYTL5	synaptotagmin-like 5 (sytl4 mouse)	
TBC1D9	TBC1 domain family, member 9 (with GRAM domain)	
TNNC1	troponin C type 1 (slow)	
TYRO3	TYRO3 protein tyrosine kinase	

Supplementary Table 1. (a) Transcripts elevated two-fold or more during DE formation in HESC-H9 and iPSC lines 3.12 and 3.5. **(b)** Transcripts elevated in DE of both human and mouse. Transcripts elevated in HESC-DE were compared to transcripts in mouse e7.5 dissected DE and ones that were elevated in both are shown. The mouse data were from table S1 in [42] and from additional analyses. There were several transcripts that were expressed in HESC-DE and are reported to be expressed in mouse embryonic DE (Reference), however these transcripts were not found to be differentially expressed in mouse DE by microarray analysis.

Supplementary Table 2a. Frequency of spheroid formation from HESC-H9

Days of GF treatment (H9 hESCs)	**Total # organoids FGF4 treated** (# organoids/wells counted)	**Average # organoids per well** FGF4 treated	**Total # organoids FGF4+Wnt3a treated** (# organoids/ wells counted)	**Average # organoids per well** FGF4+Wnt3a treated
2 days (48h)	0/5	**0**	10/10	**1**
3 days (72h)	0/5	**0**	150/10	**15**
4 days (96h)	44/5	**8.8**	322/10	**32.2**
5 days (120h)	19/4	**4.75**	100/8	**12.5**

Supplementary Table 2b. Frequency of spheroid formation from iPSC-3.5

Days of GF treatment (iPSCs)	**Total # organoids FGF4 treated** (# organoids/ wells counted)	**Average # organoids per well** FGF4 treated	**Total # organoids FGF4+Wnt3a treated** (# organoids/wells counted)	**Average # organoids per well** FGF4+Wnt3a treated
2 days (48h)	0/4	**0**	0/10	**0**
3 days (72h)	10/4	**2.5**	229/10	**22.9**
4 days (96h)	14/4	**3.5**	206/10	**20.6**

Supplementary Table 2c. Comparison of spheroids formation in different ESC and iPSC lines.

	iPSC3.5	**iPSC3.6**	iPSC18.3	**iPSC18.4**	iPSC20.1	H1	H9
2 days (48h)	2	**0**	3	**0**	1	2	0
3 days (72h)	20	**1**	28	**2**	37	33	37
4 days (96h)	0	**0**	37	**0**	24	38	42

Supplementary Table 2. Generation of hindgut spheroids was tracked for **(a)** days 2-5 following growth factor treatment for H9 hESCs or **(b)** days 2-4 of growth factor treatment for iPSCs**.** Definitive endoderm was treated with either 500ng/mL FGF4 alone or 500ng/mL FGF4+Wnt3a. For both HESCs and iPSCs, hindgut spheroids formed much more robustly under FGF4+Wnt3a conditions. Control cultures or ones treated with Wnt3a alone never formed spheroids. Over the course of 4 days, FGF4+Wnt3a treated H9 endoderm generated an average of 4.5 fold more spheroids than that treated with FGF4 alone. Similarly, FGF4+Wnt3a treated iPSC endoderm generated an average of 7.25 fold more spheroids than that treated with FGF4 alone. **(c)** Comparison of hindgut spheroid formation between different HESC lines (H1 and H9) and iPSC lines. All lines were split, differentiated and analyzed in parallel to avoid experimental variability.

Supplementary Table 3. Primary and Secondary Antibodies.

Primary Antibody	**Source**	**Dilution**
Mouse anti-Phosphohistone H3	Abcam	1:500
Rat anti-BrdU	Abcam	1:500-1:1000
Rabbit anti-Ki67	Dako	1:500
Goat anti-Sox17	R&D Systems	1:500
Mouse anti-FoxA2	Novus Biologicals	1:500
Goat anti-Villin	Santa Cruz	1:200-1:500
Mouse anti-Cdx2	BioGenex	1:500
Rabbit anti-ChromograninA	ImmunoStar	1:1000
Rabbit anti-Mucin (MUC2)	Santa Cruz	1:200
Rabbit anti-Lysozyme	Zymed Laboratories	1:1000
Rat anti-Klf5	Dr. Ichiro Manabe	1:2000
Rabbit anti-Sox9	Millipore	1:1000
Rabbit anti-Albumin	Sigma	1:1000
Rabbit anti-Laminin	Abcam	1:500
Mouse anti-E-Cadherin	BD Biosciences	1:500
Mouse anti-Smooth Muscle Actin	Millipore	1:500
Mouse anti-Neurogenin 3	DSHB	1:100
Goat anti-Vimentin	Santa Cruz	1:1000
Goat anti-Pdx1	Abcam	1:5000
Goat anti-Dpp4	R&D Systems	1:500
Rabbit anti-Phosphohistone H3	Cell Signaling	1:500
Goat anti-Gata4	Santa Cruz	1:200
Rabbit anti-Gata6	Santa Cruz	1:200
Rabbit anti-Nanog	Cosmo Bio. Co.	1:2500
Chicken anti-DNMT3b	Millipore	1:1000
Mouse anti-Tra 1-60	Millipore	1:500
Mouse anti-Tra 1-81	Millipore	1:500
Secondary Antibody	**Source**	**Dilution**
Goat anti-guinea pig Cy5	Jackson Immuno	1:500
Goat anti-rabbit Cy5	Jackson Immuno	1:500
Goat anti-rabbit Cy3	Jackson Immuno	1:500
Goat anti-mouse Cy3	Jackson Immuno	1:500
Goat anti-mouse 488	Invitrogen	1:500
Goat anti-rabbit 488	Invitrogen	1:500
Donkey anti-guinea pig Cy5	Jackson Immuno	1:500
Donkey anti-rabbit Cy5	Jackson Immuno	1:500
Donkey anti-rabbit Cy3	Jackson Immuno	1:500
Donkey anti-mouse Cy3	Jackson Immuno	1:500
Donkey anti-rabbit 488	Invitrogen	1:500
Donkey anti-mouse 488	Invitrogen	1:500

Supplementary information references

39 Higashihori, N., Song, Y. & Richman, J. M. Expression and regulation of the decoy bone morphogenetic protein receptor BAMBI in the developing avian face. *Dev Dyn* **237**, 1500-1508, doi:10.1002/dvdy.21529 (2008).

40 Schultheiss, T. M., Burch, J. B. & Lassar, A. B. A role for bone morphogenetic proteins in the induction of cardiac myogenesis. *Genes Dev* **11**, 451-462 (1997).

41 Lopez-Sanchez, C., Puelles, L., Garcia-Martinez, V. & Rodriguez-Gallardo, L. Morphological and molecular analysis of the early developing chick requires an expanded series of primitive streak stages. *J Morphol* **264**, 105-116, doi:10.1002/jmor.10323 (2005).

42 Gu, G. *et al.* Global expression analysis of gene regulatory pathways during endocrine pancreatic development. *Development* **131**, 165-179 (2004).

43 Zhao, R. *et al.* GATA6 is essential for embryonic development of the liver but dispensable for early heart formation. *Mol Cell Biol* **25**, 2622-2631 (2005).

44 Filosa, S. *et al.* Goosecoid and HNF-3beta genetically interact to regulate neural tube patterning during mouse embryogenesis. *Development* **124**, 2843-2854 (1997).

45 Thomas, P. Q., Brown, A. & Beddington, R. S. Hex: a homeobox gene revealing peri-implantation asymmetry in the mouse embryo and an early transient marker of endothelial cell precursors. *Development* **125**, 85-94 (1998).

46 Oulad-Abdelghani, M. *et al.* Stra3/lefty, a retinoic acid-inducible novel member of the transforming growth factor-beta superfamily. *Int J Dev Biol* **42**, 23-32 (1998).

47 Norris, D. P., Brennan, J., Bikoff, E. K. & Robertson, E. J. The Foxh1-dependent autoregulatory enhancer controls the level of Nodal signals in the mouse embryo. *Development* **129**, 3455-3468 (2002).

48 Saijoh, Y. *et al.* Left-right asymmetric expression of lefty2 and nodal is induced by a signaling pathway that includes the transcription factor FAST2. *Mol Cell* **5**, 35-47, doi:S1097-2765(00)80401-3 [pii] (2000).

49 Hart, A. H. *et al.* Mixl1 is required for axial mesendoderm morphogenesis and patterning in the murine embryo. *Development* **129**, 3597-3608 (2002).

50 Acampora, D. *et al.* Visceral endoderm-restricted translation of Otx1 mediates recovery of Otx2 requirements for specification of anterior neural plate and normal gastrulation. *Development* **125**, 5091-5104 (1998).